Report

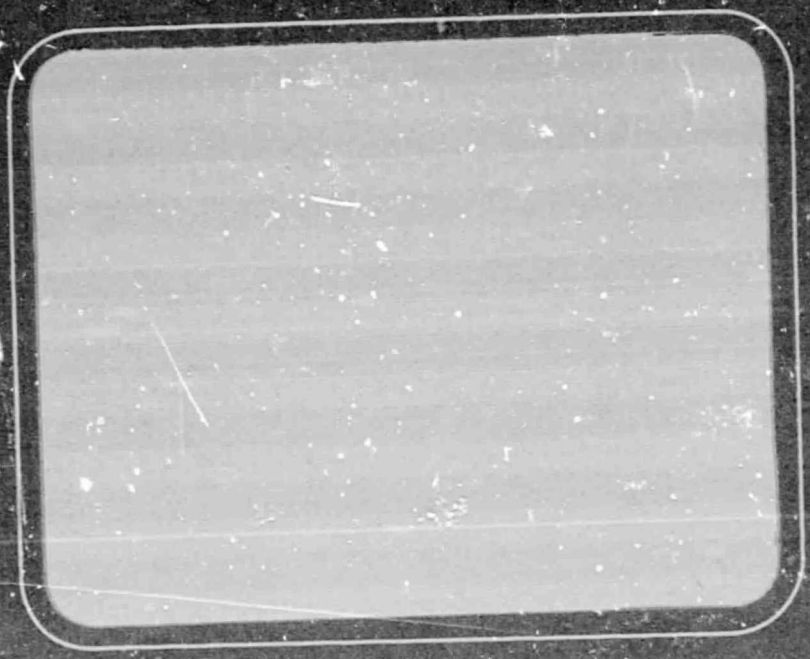

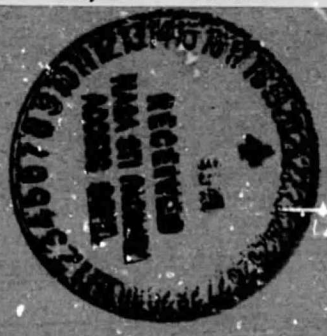

FINAL REPORT

on

EVALUATION OF SSME HIGH PRESSURE LIQUID OXYGEN TURBOPUMP BEARINGS

to

GEORGE C. MARSHALL SPACE FLIGHT CENTER
MAESHALL SPACE FLIGHT CENTER, ALABAMA

April 6, 1979

by

K. F. Dufrane and J. W. Kannel

BATTELLE
Columbus Laboratories
505 King Avenue
Columbus, Ohio 43201

TABLE OF CONTENTS

LIST OF TABLES

LIST OF FIGURES

TABLE OF CONTENTS
(Continued)

EVALUATION OF SHUTTLE TURBOPUMP BEARINGS

by

K. F. Dufrane and J. W. Kannel

April 6, 1979

INTRODUCTION

NASA and the Rockeydyne Division of Rockwell International are developing long-life turbopumps for use on the shuttle. Because of the re-usable design of the shuttle, lifetimes of 27,000 seconds (7.5 hours) are being sought. Since most turbopumps to date have operated for periods of on the order of only hundreds of seconds, the desired lifetime is a significant extension of technology. The mainshaft support bearings are of particular concern in this regard. In support of these efforts, Battelle's Columbus Laboratories (BCL) undertook the one month study described in this report to examine a used pair of bearings. The examination was similar to that conducted previously on a set of bearings under contract NAS8-32987.

The two bearings examined were run in high pressure turbopump (HPTP) No. 9103. A total of 5403 seconds of running were accumulated, most of which was at 100 percent output (approximately 28,000 rpm). The running included 19 starts. The bearings are angular-contact ball bearings, applied as a preloaded pair, locked to the shaft, inner race rotating, with the outer races permitted to move unrestrained axially over a limited distance (i.e., the bearings are intended to provide radial location only). The bearings examined in the study were from the turbine end and were identified as follows:

Bearing Position	Bearing Serial Number	Bearing Part Number
3	8517903	02602-2DRS007955-001
4	8517900	02602-2DRS007955-001

Battelle's specific objectives in the study were:

(1) Perform a visual, scanning electron microscopy (SEM), metallurgical, and dimensional analysis of the bearings (as needed).
(2) Estimate the nature and magnitude of the loads applied to the bearings based on the contact patterns.
(3) Recommend further analytical efforts required (including an estimate of magnitude of costs) and any design, material, or lubrication changes that will improve the durability of the bearings.

SUMMARY AND RECOMMENDATIONS

Examination of the bearings produced conclusive evidence that a very high axial load (at least 27,000 N [6000 pounds]) had been applied to bearing 8517903 during a significant portion of the service time. The high loads caused serious ball and race wear and surface fatigue pitting. In all likelihood, continued operation of this bearing with the high axial load would have caused increasing deterioration and catastrophic failure. In contrast, bearing 8517900 showed much less deterioration and probably had experienced only the axial loads deliberately applied by the preload spring. Bearing 8517900 represents the best-case operation with the loads controlled to the levels intended in the design.

Fatigue life calculations on bearing 8517903 with an axial load of 27,000 N (6000 pounds) showed the intolerance of the bearing to such load levels. The predicted L_1 fatigue life was only 20 minutes (1200 seconds). This extremely short life indicates that the bearing was grossly overloaded. The theoretical prediction was partially confirmed by the presence of surface fatigue spalls in the ball-contact band of the inner race. Continued service would enlarge these pits, and their presence, along with the wear bands on the balls, would result in increasingly rough bearing operation. Eventually the retainer would deteriorate and complete catastrophic failure would follow.

This probably would have occurred in a relatively short additional time of operation.

Based on these findings, we make the following specific recommendations:

(1) Make the assembly or design modifications required to insure that no high axial load levels are applied to the bearings. The high load experienced by bearing 8517903 must have resulted from an outer race lock-up or operation at the extreme limits of axial travel. Both possibilities should be explored to identify the cause.

(2) Reduce bearing curvature from 0.53 to 0.52 on both races to reduce contact stress and enhance transfer film lubrication.

(3) Initiate a bearing design program at Battelle to include:

- Transfer film evaluation
- Bearing pretreatment evaluation
- Bearing configuration design analyses
- Bearing test recommendations for Rocketdyne [see (5) below] to develop reliable bearing tests that simulate actual operation.

(4) Conduct a research evaluation on the hydrogen pump bearings of the type presented here for the oxygen pump bearings.

(5) Conduct a matrix of bearing tests at Rocketdyne to optimize bearings for both the hydrogen and the oxygen pumps. Parameters should include:

- Race curvature as per (2) above
- Pretreatment of bearing components
- Precoatings such as sputtered films of MoS_2.

COMPONENT INSPECTION

Bearing 8517903 Examinations

Races

The inner race of bearing 8517903 showed evidence of considerable distress when examined at low magnifications. Three distinct continuous bands were present, which resulted from contact with the balls. Extending from the chamfer on the largest inner race diameter was a smoothly worn band approximately 2.97 mm (0.117 inch) wide. Its color was grey to brown in patches, which probably was a combination of oxide layers and transferred TFE from the retainer. By placing a ball from the bearing in this portion of the race, the use of transmitted light showed that the wear (and possibly deformation) was sufficient to change the race curvature to match that of the ball. Extending away from the smoothly worn band was a 2.08 mm (0.082 inch)-wide band consisting of numerous fine pits. Finally, a third polished narrow band 0.69 mm (0.027 inch) wide completed the ball contact track. Since the bands did not vary significantly in width or location, apparently the synchronous radial loads were not high compared to the axial loads in service.

Scanning electron microscopy (SEM) was used to examine the details of the race wear. Typical areas are presented in Figure 1. In Figure 1(a), the larger pits appear to be shallow fatigue spalls that progressed from right to left in the micrograph. The wear features shown in Figure 1(b) were aligned with the direction of rolling. The surface consisted of a series of furrows, which were probably caused by mild adhesive wear with the balls, and scattered fine pits.

Metallographic sections were prepared across the inner race to measure the depth of the spalls, to determine whether any fatigue cracks extended into the bulk material, and to measure the microhardness as an indication of maximum operating temperature. A micrograph of a section through one spall is presented in Figure 2. The spalled region was approximately 2 μm (80 micro-inches) deep. The micrograph also shows that a crack had progressed into the surface and to the right from the bottom of the spall. The crack progressed along the carbide-matrix interface or through the carbides themselves. This

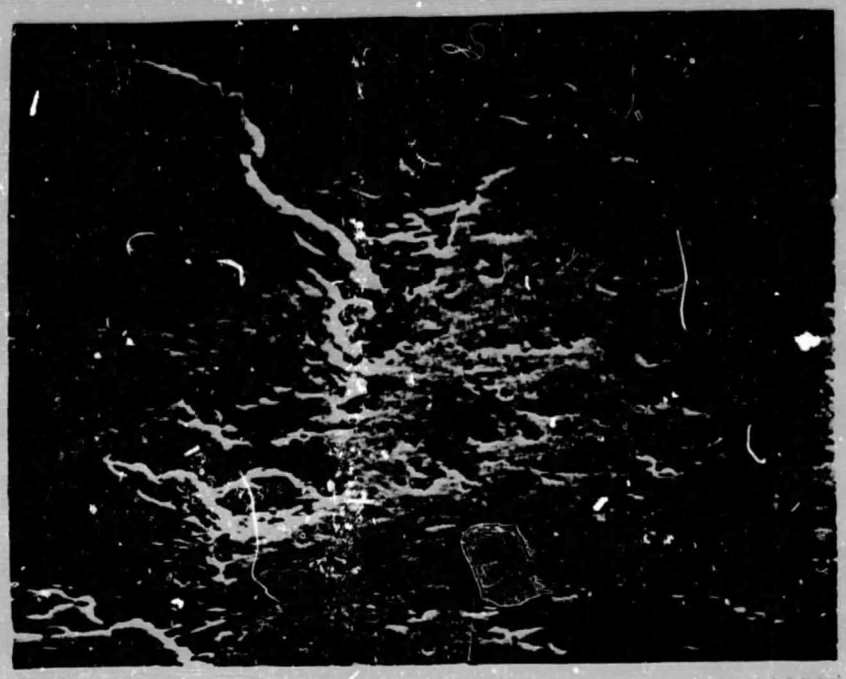

22039 1000X

(a) Pitted Band Area

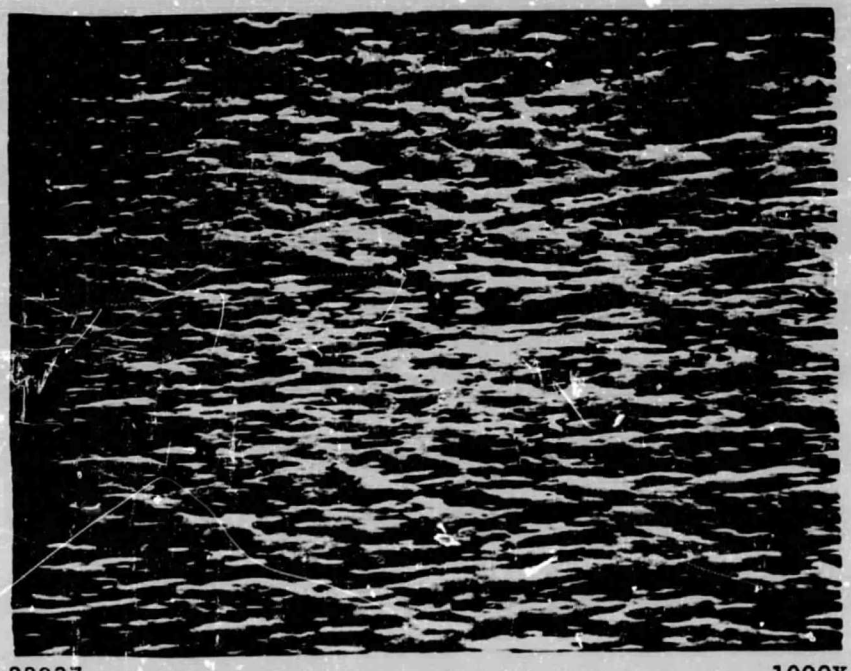

22037 1000X

(b) Worn Band Area

FIGURE 1. SCANNING ELECTRON MICROGRAPHS OF DAMAGE TO INNER RACE OF BEARING 8517903

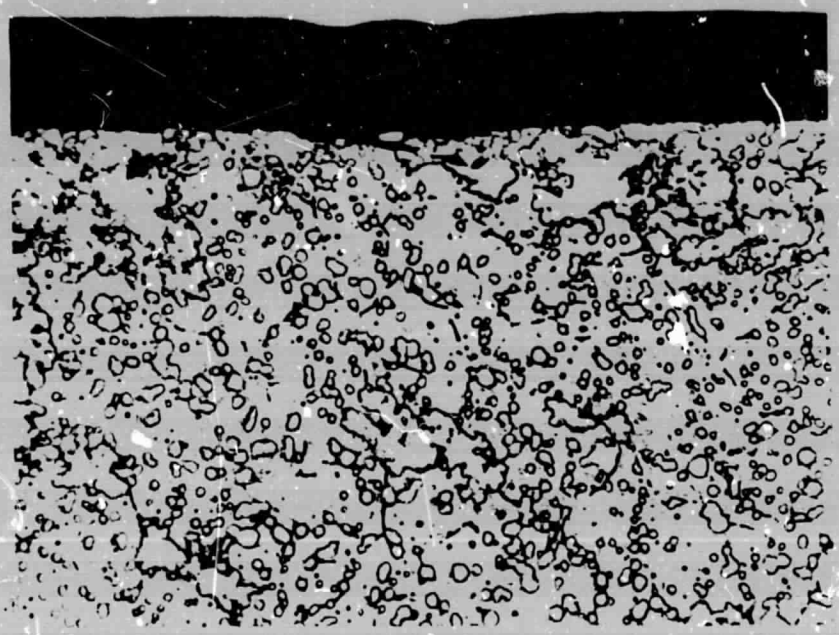

FIGURE 2. MICROGRAPH SHOWING CROSS SECTION OF SURFACE SPALL AND CRACK PROPAGATING FROM THE SPALL ON INNER RACE OF BEARING 8517903

spall probably would have tripled in width and reached a depth of 6.3 μm (250 microinches) in a short time of additional running. Microhardness readings taken on the metallographic section just under the worn surfaces could detect no reduction in hardness from the bulk hardness. Since 440 C stainless steel requires a tempering temperature of 204 C (400 F) to begin to reduce hardness, temperatures of this level were not attained by this inner race in service.

The outer race of bearing 8517903 also had continuous distinct bands of wear and pitting resulting from contact with the balls. Mild wear, generally not entirely through the original grinding scratches, extended from 10 mm (0.040 inch) from the thrust-side chamfer with a width of 3.12 mm (0.123 inch). The edge of the mild-wear track away from the chamfer was defined by a continuous row of pits with depths of approximately 0.013 mm (0.0005 inch). Alongside the row of pits was a worn band 1.1 mm (0.042 inch) in width consisting of mild wear and fine pitting. Finally, a smooth, polished band 0.64 mm (0.025 inch) in width completed the total area of ball contact. All of the bands were continuous in width and location around the race, which indicates that no significant non-synchronous (stationary) radial load was experienced during running.

SEM micrographs of the outer race wear areas are shown in Figure 3. The pitting in Figure 3(a) was a combination of straight-sided pits (probably localized fatigue pits) and shallow rounded pits (probably caused by indentation by the debris from the fatigue pits). The pitting in the mildly worn band, Figure 3(b), was similar to that in the heavily pitted band of Figure 3(a), except that the concentration of pits was much lower. Also, the areas between the pits were smooth and polished, which gave the appearance in optical microscopy of this band having had much milder wear.

Balls

The balls from bearing 9517903 all had several small-circle (non-equatorial) bands intersecting at random angles to each other. Transmitted light with a ball placed against the inner race showed the bands to have a significant wear depth (measurements described below in section on cross-race curvature and ball roundness measurements). The balls (including most of the bands) had a blue to grey color cast, which was suggestive of oxidation of

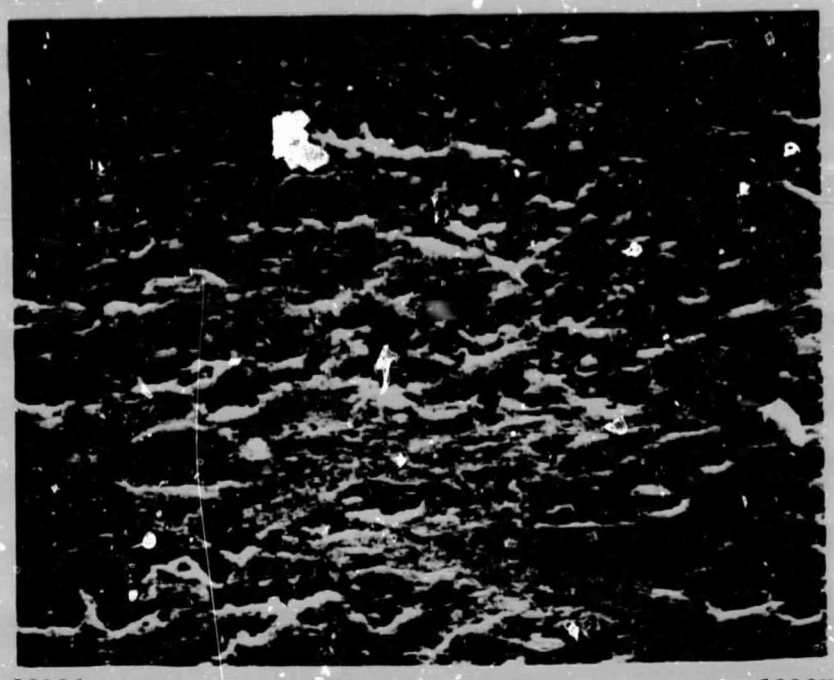

22036 1000X

(a) Heavily Pitted Band

22035 1000X

(b) Mild Wear Band

FIGURE 3. SCANNING ELECTRON MICROGRAPHS OF WORN AREAS OF OUTER RACE OF BEARING 8517903

the surface. A few of the bands were metallic in color, which indicates that these bands probably formed last and the surface coloration was worn away during their formation.

Examination of the balls by SEM found the worn bands to have the appearance shown in the micrograph in Figure 4. The wear probably occurred by an adhesive mechanism combined with some pitting. Subsequent running over the area then flattened the raised portions, which resulted in the raised featureless areas in Figure 4. Areas between the bands were very mildly worn with remnants of original finishing scratches still present.

Metallographic sections were made through the balls to examine the microstructure under the bands. At lower magnifications, Figure 5(a), the bands were seen to have nearly flat areas worn on the overall ball curvature. The straight reference line was placed in Figure 5(a) above the flat region. to demonstrate its length and distinct change from the normal ball curvature. At higher magnifications, Figure 5(b), the microstructure was seen to be unchanged from normal near the surface as a result of the band formation. Microhardness readings also confirmed that the steel had not been tempered as a result of local overheating when the band was formed.

Retainer

The retainer from the bearing 8517903 was found to be in excellent condition with only very mild wear on the outer guiding surface and in the ball pockets. There was no evidence of delamination, distortion, or heavy wear as a result of service. A slight lip of TFE was found in the pockets on the outer diameter, which apparently resulted from a finishing step when the retainer was being manufactured.

Talysurf profiles were taken across the ball pockets to measure the depth of wear from contacting the balls. Representative traces are shown in Figure 6. The lip at the outer diameter can be clearly seen as the raised portion at the left of the traces. The maximum wear depth was found to be approximately 0.025 mm (0.001 inch) which is quite tolerable.

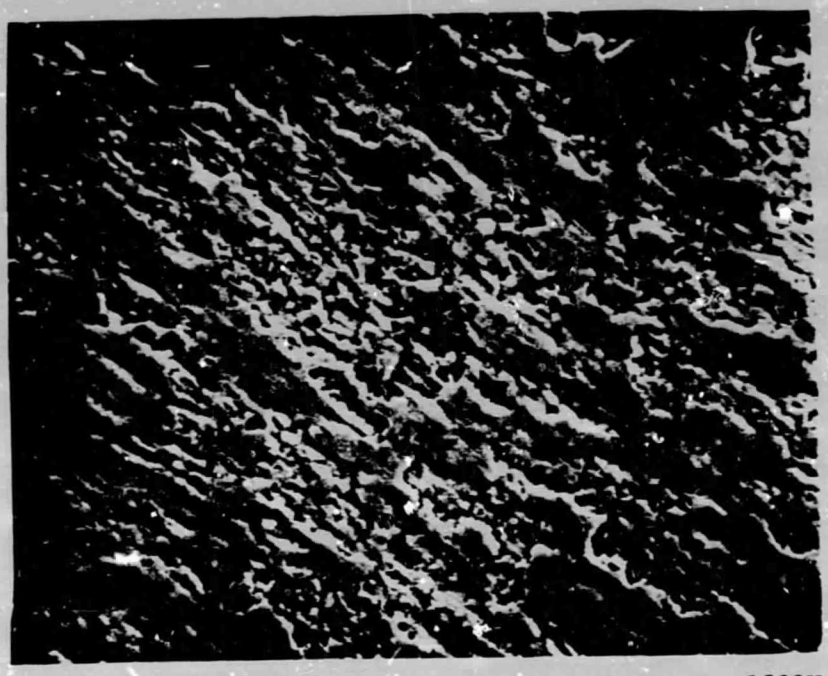

22045 1000X

FIGURE 4. SURFACE OF BALL FROM BEARING 8517903 SHOWING WEAR IN BAND AREA

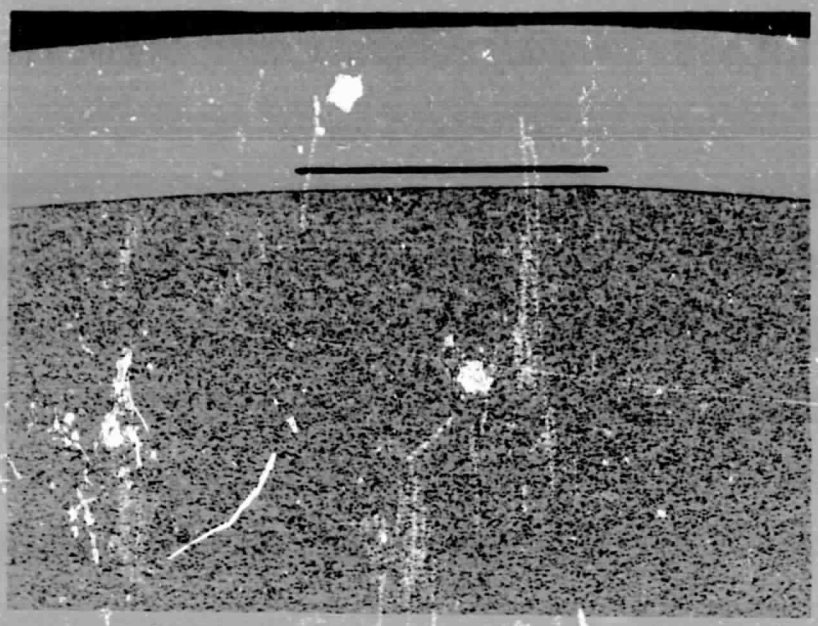

7J987 100X

(a) Flat worn area of band

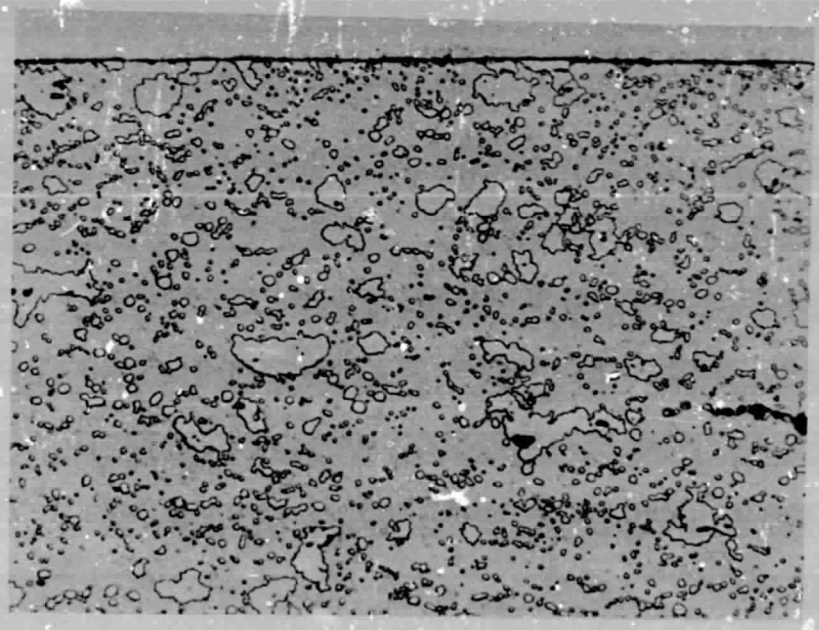

7J986 750X

(b) Microstructure under Band

FIGURE 5. METALLOGRAPHIC CROSS SECTIONS OF BAND AREA ON BALL FROM BEARING 8517903

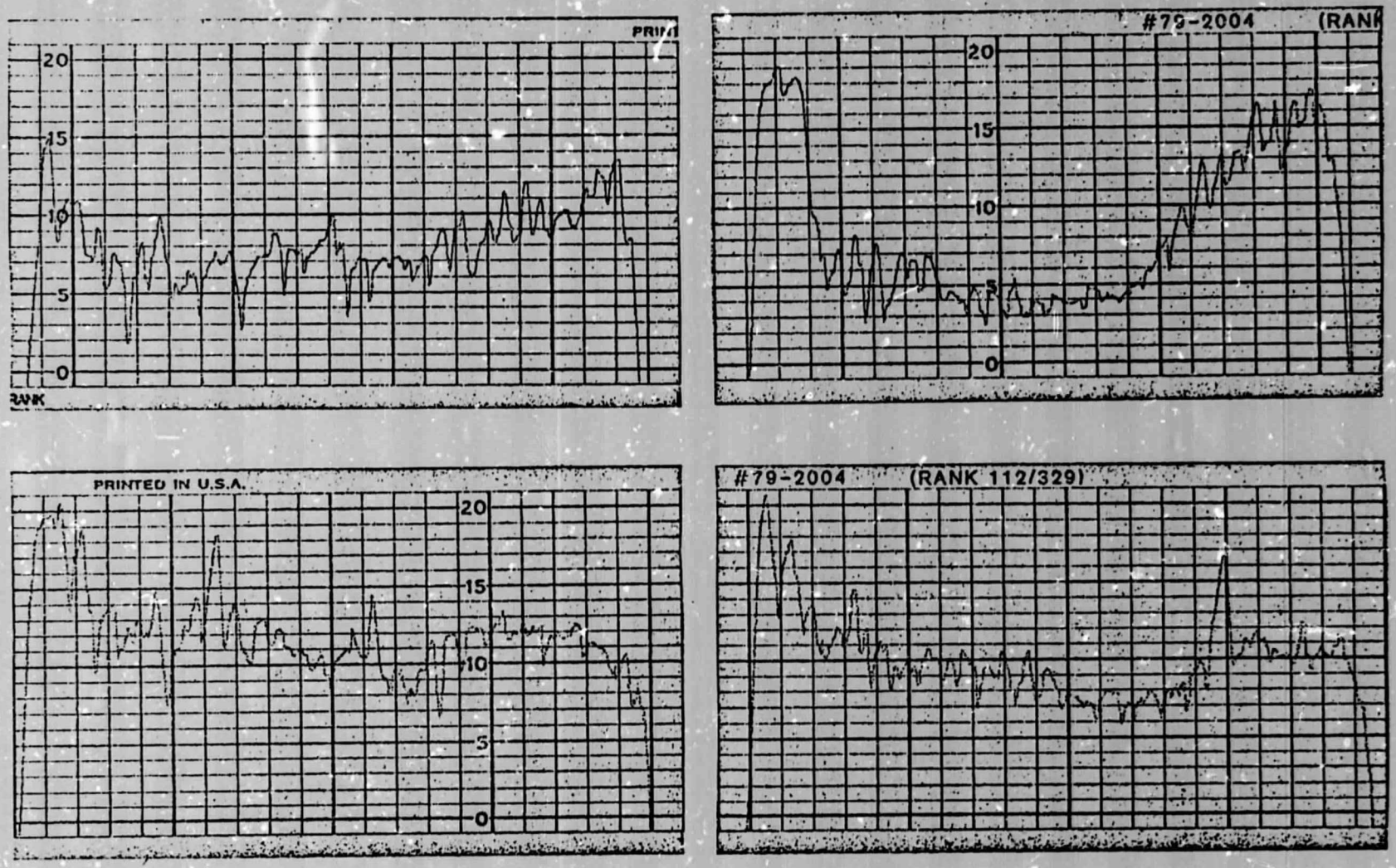

FIGURE 6. PROFILES OF WEAR AREAS OF RETAINER BALL POCKETS FROM BEARING 8517903
MAGNIFICATIONS, MINOR DIVISIONS,
VERTICAL : 5.0 μm (200 microinches)
HORIZONTAL: 0.25 mm (.010 inch)

Bearing 8517900 Examinations

Races

The inner race of bearing 8517900 showed evidence of very mild wear and no distress as a result of its service time. The ball contact track was continuous and uniform in width and location. The track was approximately 4.1 mm (0.160 inch) in width and was located with one edge approximately 1.1 mm (0.045 inch) from the chamfer. Since original grinding scratches were faintly visible on most of the track width, the depth of wear was apparently on the order of the depth of the scratches. There was also some evidence of race denting from soft debris, but the dents were of minor depth and randomly scattered. An area near the center of the band was darker in color, which was possibly the result of deeper wear or more extensive transfer of TFE.

The outer race of bearing 8517900 was also mildly worn in a ball contact path that did not vary in width or location. It had one edge located approximately 2.8 mm (0.110 inch) from the edge of the chamfer on the thrust side with a width of approximately 3.6 mm (0.140 inch). Similar to its mating inner race, remnants of original grinding scratches were present in much of the ball contact path, which is associated with mild wear. Scattered soft debris dents were also present on the outer race ball-contact track. An SEM micrograph of an area in the ball contact path is shown in Figure 7. The surfaces consist mostly of very fine pits with scattered larger pits, which may have resulted from debris.

Balls

The balls from bearing 8517900 were very mildly worn with equatorial bands on most of them. Three balls showed small-circle bands. However, examination by light microscopy at 500X showed that these bands consisted primarily of transferred small patches of brown material, which was probably TFE. Otherwise, the balls showed evidence of scattered fine pitting, similar to the races, over most of their surface.

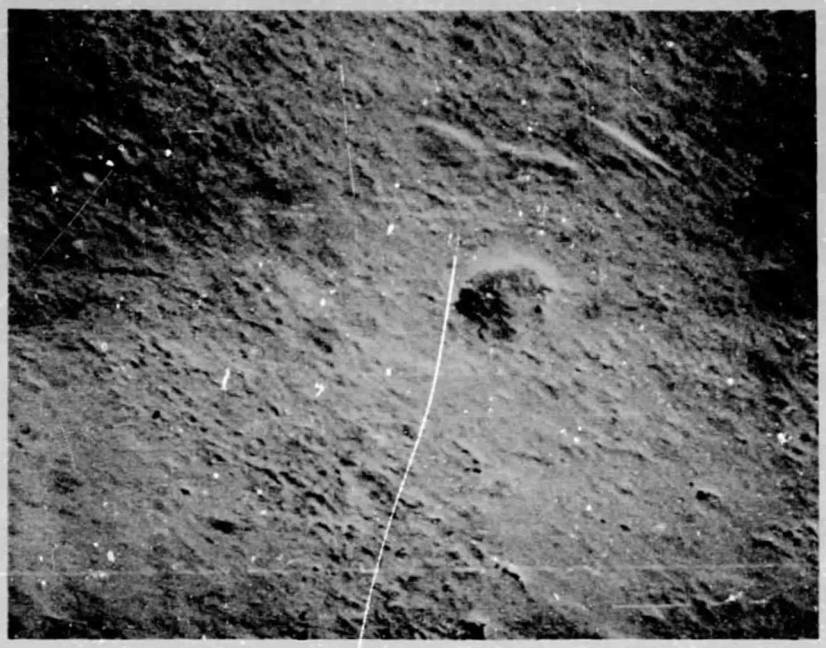

22046 1000X

FIGURE 7. BALL CONTACT PATH ON OUTER RACE OF BEARING 8517900

Retainer

The retainer from bearing 8517900 was in excellent condition and had only minor wear areas in the ball pockets. There was no evidence of distress as a result of service. Stylus profilometer traces across the ball pocket wear areas are shown in Figure 8. A raised lip was also present at the outer diameter surface of the ball pocket of this retainer, which can be seen at the left of Figure 8. The wear depth appeared to be a maximum of less than 0.025 mm (0.001 inch).

Cross-Race Curvature and Ball Roundness Measurements

Bearing 8517903

A Talyrond roundness measuring instrument was used to attain cross-race curvature profiles on the races and roundness measurements on the balls. For the races, the stylus diameter was set by gage blocks to be twice the specified race radius of 6.731 mm (0.2650 inch). Adjustments within the radius tolerance were found to be adequate to match the curvature.

Shown in Figure 9 are the traces attained on the races from bearing 8517903. The outer race, Figure 9(a), showed a groove approximately 5 μm (200 microinches) in depth near the center of the race. Since the area of the groove appeared to be completely unworn by microscopic examinations, the groove probably was produced by the original manufacturing. However, the groove measuring 1.27 μm (50 microinches) deep corresponded to the wear track area. The area of heavy race wear was clearly visible on the profile of the inner race, Figure 9(b). A maximum wear depth of approximately 15 μm (600 microinches) was measured in the region that conformed to the curvature of the ball.

Talyrond traces of two balls from bearing 8517903 are shown in Figure 10. The depth of the wear bands below the original curvature is clearly visible. A maximum depth of approximately 11 μm (450 microinches) was measured. Since the Talyrond magnification is very high radially, the shape of the wear bands is greatly distorted. The actual shape was shown to be more nearly flat areas in the metallographic cross sections. Measurements of

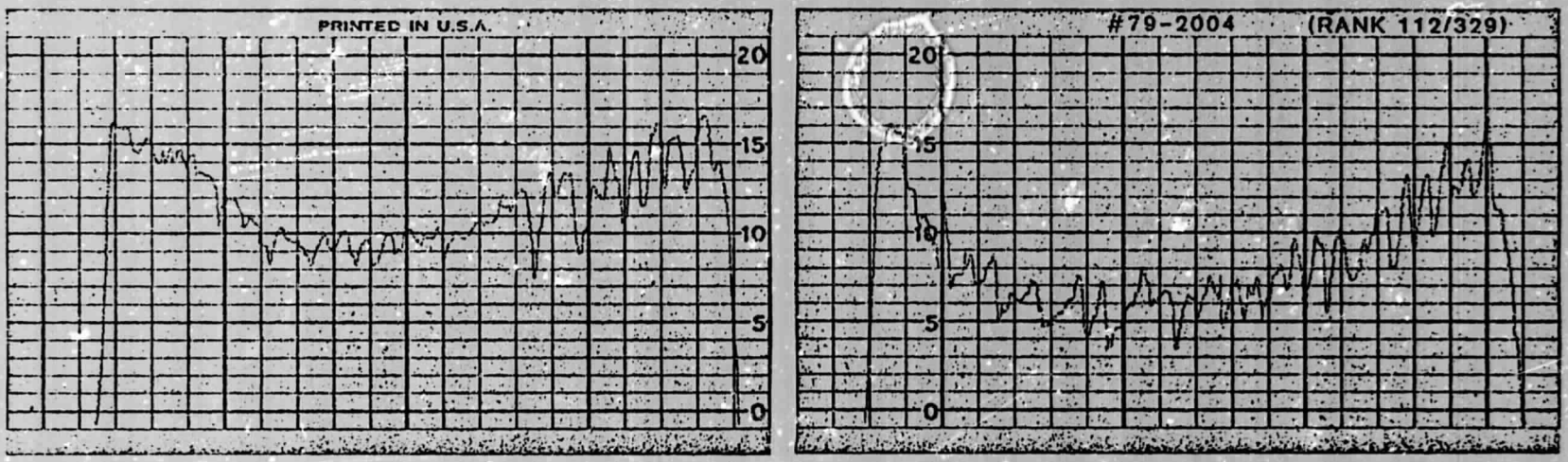

FIGURE 8. PROFILES OF WEAR AREAS IN BALL POCKETS OF RETAINER FROM BEARING 8517900
MAGNIFICATIONS, MINOR DIVISIONS,
VERTICAL : 5 μm (200 microinches)
HORIZONTAL: 0.25 mm (0.010 inch)

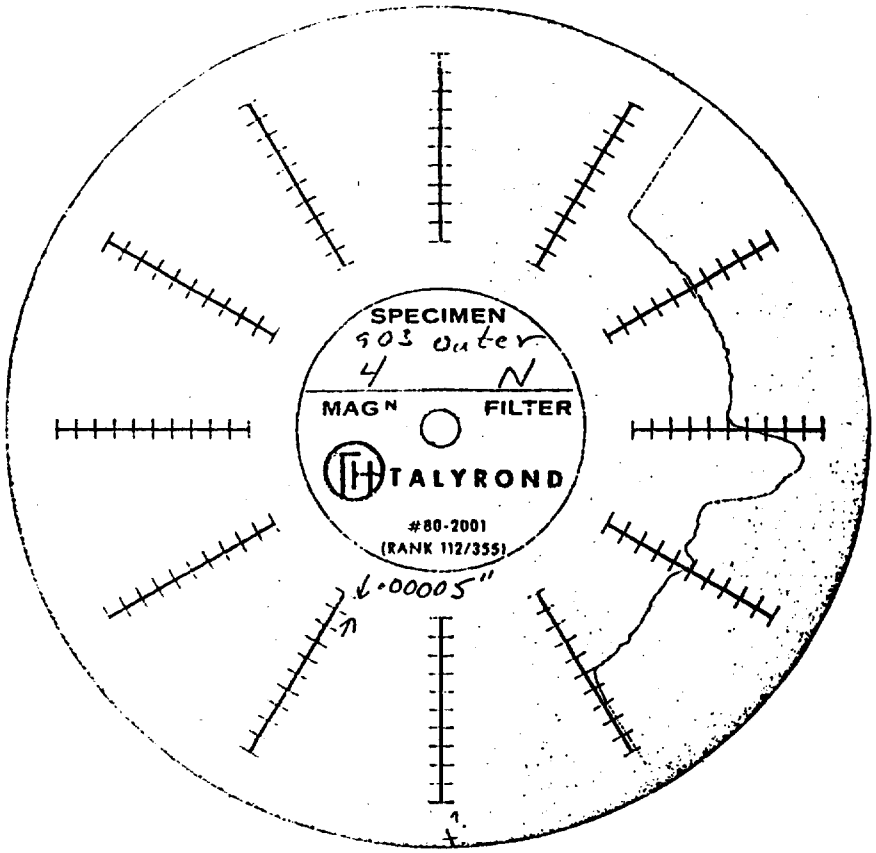

(a) Outer Race

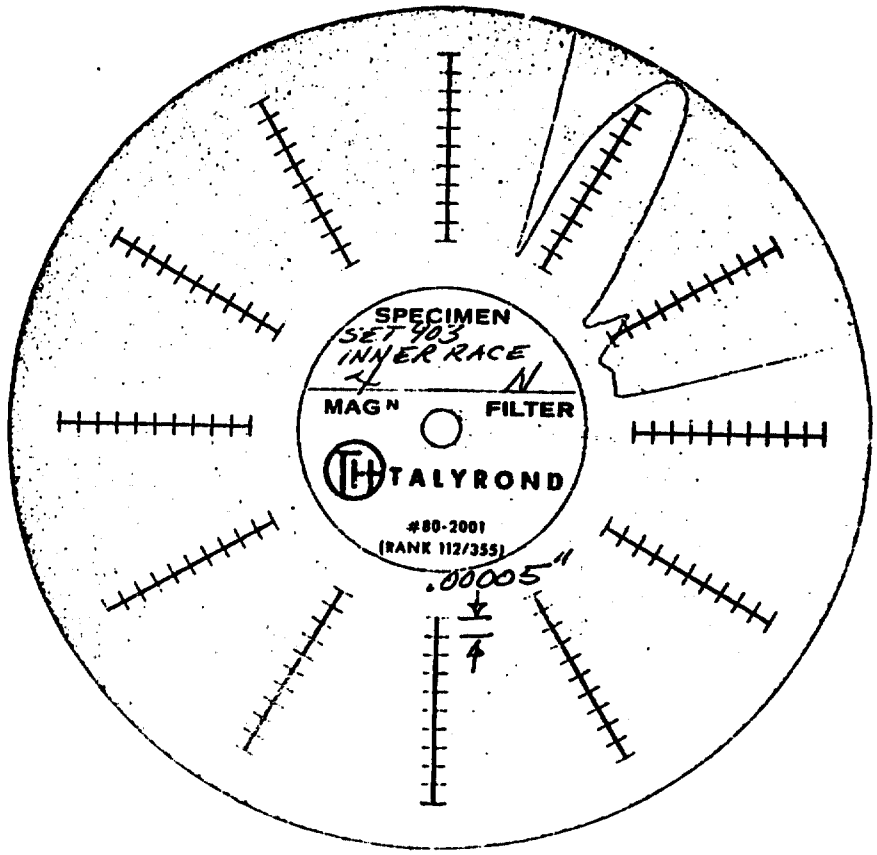

(b) Inner Race

FIGURE 9. CROSS-RACE CURVATURES OF RACES FROM BEARING 8517903
RADIAL MAGNIFICATION,
1 Division = 1.27 μm (50 microinches)

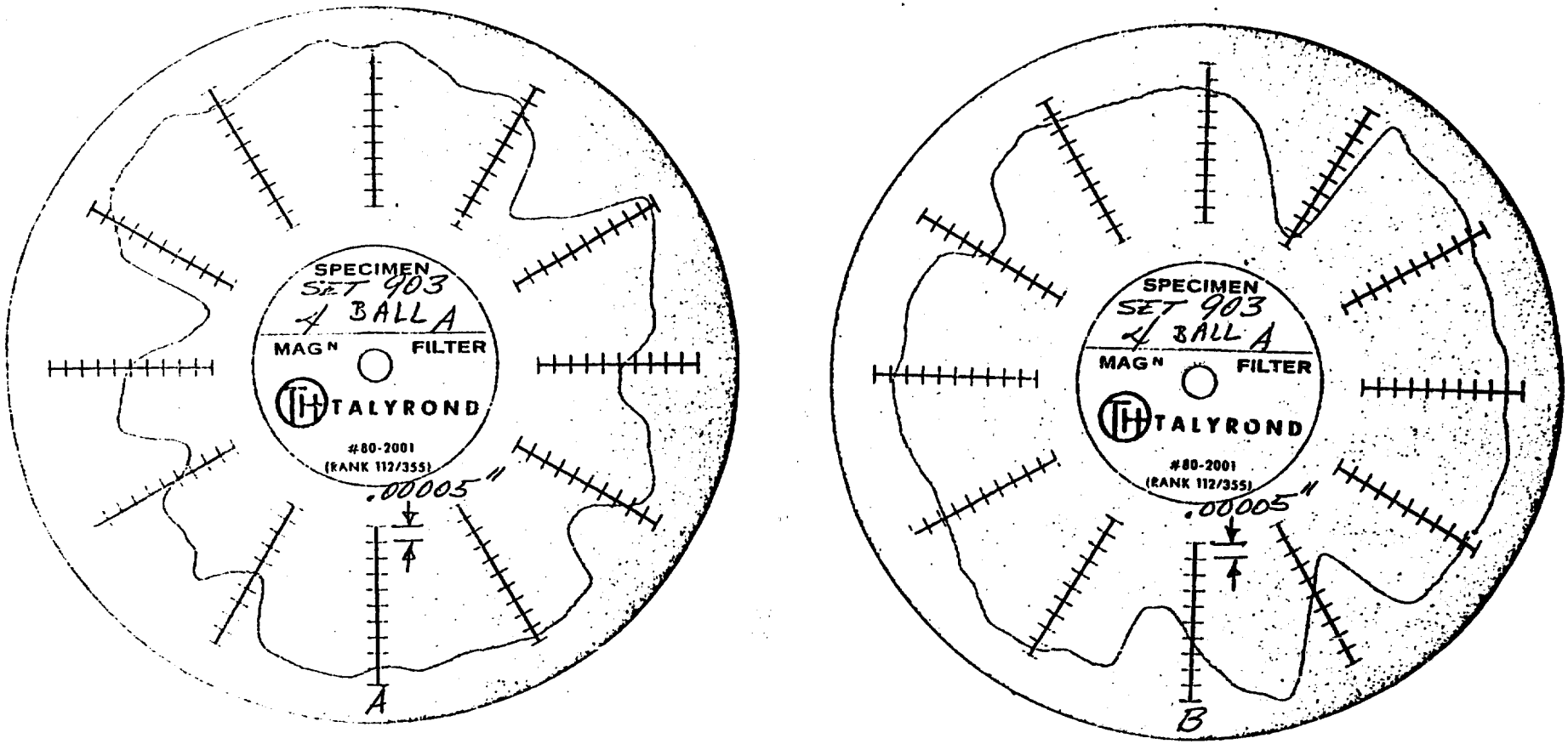

FIGURE 10. ROUNDNESS MEASUREMENTS ON TWO BALLS FROM BEARING 8517903
RADIAL MAGNIFICATION,
1 Division = 1.27 μm (50 microinches)

the angular locations of the bands showed the average included angle of the cone formed by mid-position of the bands and the center of the ball was approximately 125 degrees. The average angular width of the bands was 25 degrees. The bands represent a major deterioration of the original geometry of the balls.

Bearing 8517900

Cross-race curvature measurements made on the races from bearing 8517900 are shown in Figure 11. The slight deviation from roundness on the outer race, Figure 11(a), may have been produced during manufacturing. The groove seen in Figure 11(b) on the inner races was approximately 3.8 μm (150 microinches) below the normal curvature. Since this occurred in the ball track area, it probably was caused by wear from the balls.

The roundness traces attained on two balls from bearing 8517900 are shown in Figure 12. The difference between the maximum and minimim diameters of the ball in the upper trace was approximately 3.4 μm (135 microinches). Since these balls were very mildly worn in local bands only (whose planes were oriented perpendicular to the plane of the chart), this out-of-roundness was probably present from manufacturing. This deviation is well out of tolerance for balls used in precision bearings. The second ball, in the lower chart, showed a deviation from roundness of approximately 0.64 μm (25 microinches), which is much more acceptable.

Bulk Hardness Measurements

Rockwell C hardness measurements were taken on the bearing components to determine whether the original heat treatments were within specification. The results, presented in Table 1, show all of the components to have an acceptable hardness for the application.

TABLE 1. ROCKWELL C HARDNESS READINGS OF BEARING COMPONENTS

	Inner Race	Outer Race	Ball
8517903	61	61	59
8517900	61	61	59

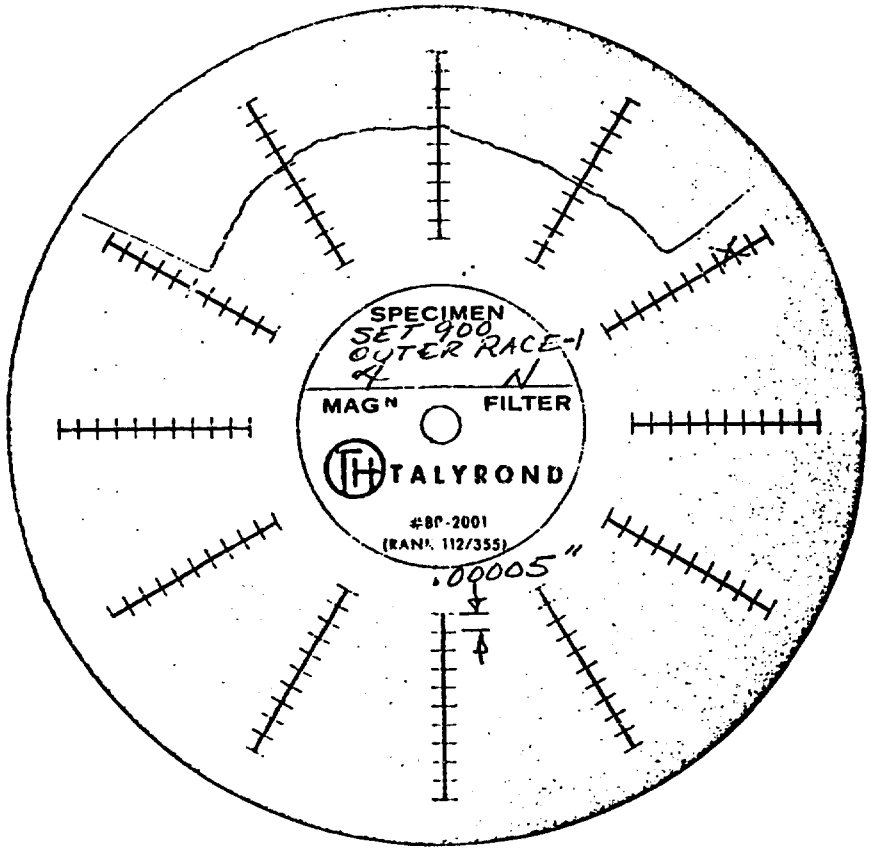

(a) Outer Race

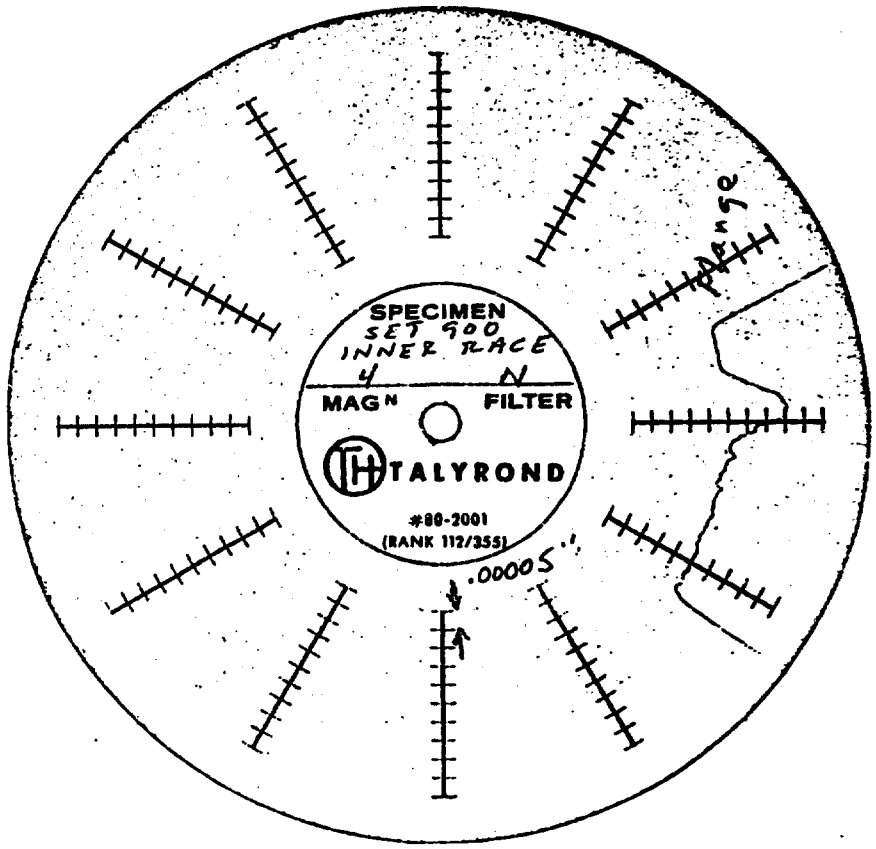

(b) Inner Race

FIGURE 11. CROSS-RACE CURVATURES OF RACES FROM BEARING 8517900
RADIAL MAGNIFICATION,
1 Division = 1.27 μm (50 microinches)

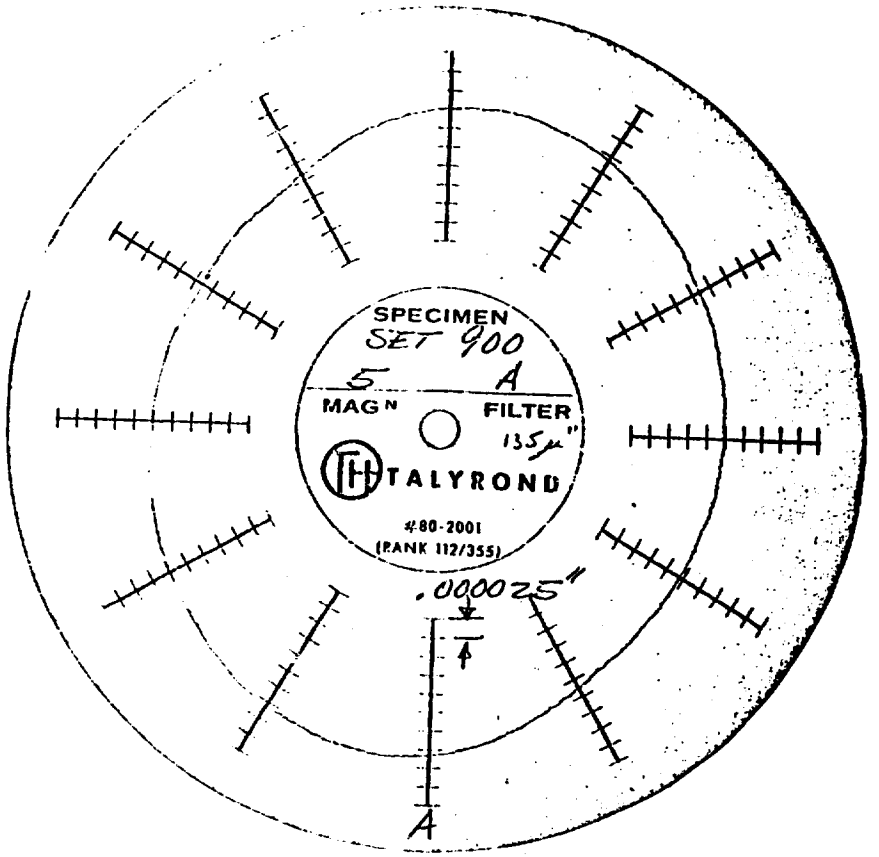

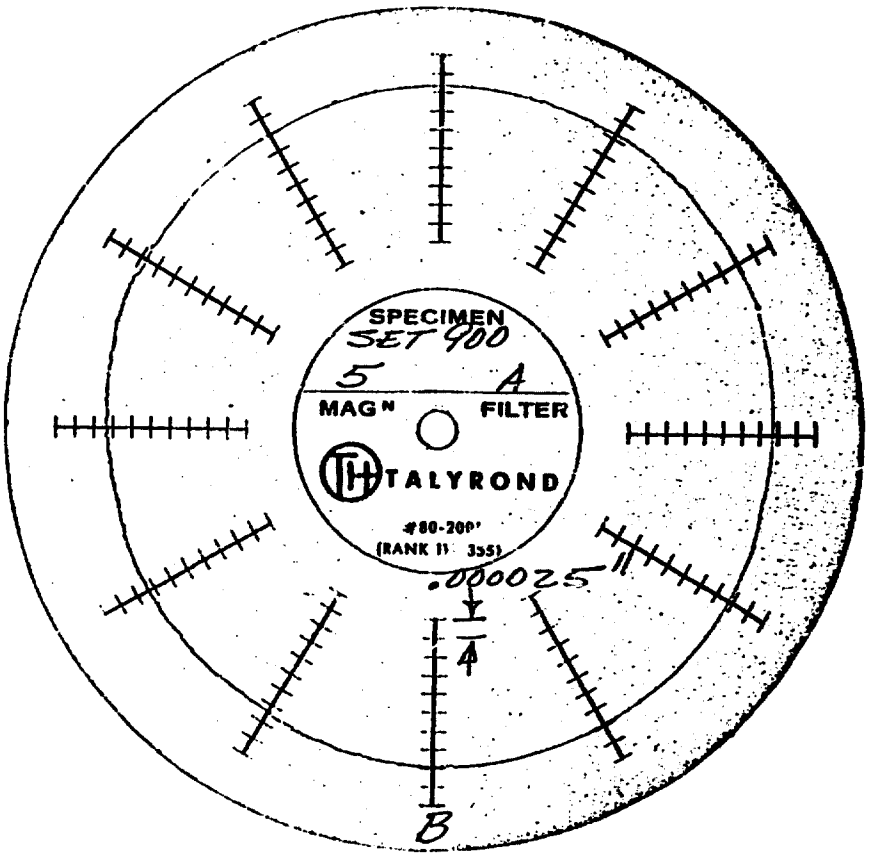

FIGURE 12. ROUNDNESS MEASUREMENTS ON TWO BALLS FROM BEARING 8517900
RADIAL MAGNIFICATION,
1 Division = 0.64 μm (25 microinches)

LOAD AND STRESS ANALYSIS

The bearing inspections have revealed that ball-race contact occurred over a wide portion of the inner races and that serious wear occurred on the inner race of bearing 8517903. In addition, numerous shallow pits, which could be suggestive of surface initiated fatigue, have been observed. These observations strongly suggest that the bearing was in a terminal condition and that continued running would have resulted in a catstrophic failure. The purpose of the following analyses is to estimate the level of loading that the bearing incurred and to guide corrective measures to enhance bearing life.

The method for bearing-load computation at Battelle involves the use of a computer program series under the general name, BASDAP. BASDAP programs can be used for static or dynamic analyses of bearings for a wide range of applications. BASDAP programs have been used in static or quasi-dynamic analyses to determine ball-race stresses and ball steady-state motions as well as analyses of dynamic behavior of the cage to determine cage stability and ball-cage loadings. The BASDAP program treats each bearing, in a set, independently.

For the project discussed herein, only a quasi-dynamic version of the BASDAP computer code was utilized. This code involves calculation of ball-race forces (inner and outer), contact pressures, contact dimensions, and contact angles as a function of:

(1) axial load

(2) radial load

(3) centrifugal load

on the bearing.

The computation technique involves first computing the load sharing between the balls in the absence of centrifugal forces. This involves a formalized trial and error (nesting type) procedure. Essentially, estimates of the axial and radial deflection of the bearing are made. The correct value of these deflections results in the correct radial and axial load. After the ball load sharing has been computed, the effect of centrifugal force on contact angle is computed. Essentially, this force causes the inner and outer race contact angles to be different from each other as well as different from the static contact angles. The method for the deflection and contact angles calculation

is modeled after the classic work of A. B. Jones*.

Results of Calculations

The characteristics of the bearing analyzed is shown in Table 2. Figure 13 shows the effect of axial load on predicted contact angle. Note here that the outer-race contact angle is more sensitive to load than is the inner. The inner-race contact angle can be assumed to be approximately 32 degrees for all conditions analyzed.

Figure 14 shows the effect of axial load on contact stress. It is obvious that increasing load seriously increases contact stresses. Also shown in Figure 14 is the upper stress limit for effective transfer-film lubrication. This limit was discussed in our previous report (November 1978) and is based on some cursory experiments in another project. The accuracy of this presumed limiting condition, thus, is unknown for the shuttle configuration, although it is by no means a conservative number. Assuming that this upper limit is accurate, it is apparent that axial loads in excess of 90,000 N (2000 pounds) can be extremely detrimental to bearing performance.

Figure 15 shows the variation in ball track width with increasing axial load. At loads of, say, 27,000 N (6000 pounds), the total track width is 4 mm (.162 inch). As will be discussed, this is equivalent to the observed track width in bearing 8517903.

Figure 16 was prepared to show the effect of loss of internal clearance on bearing stresses. It can be observed that the bearing is quite tolerant of diametral clearance losses in excess of .1 mm (.004 inch). It is unlikely, then, that clearance loss due to large inner race temperatures are a major contribution to bearing distress.

Estimation of Actual Axial Loads

Figures 17 and 18 combine the actual measurements of ball contact path locations with those contact angles and ball contact widths that give the best simultaneous fit. In this manner, an estimate can be made of the actual axial loads applied to the bearings during service.

---

*Jones, A. B., "A General Theory for Elastically Constrained Ball and Roller Bearings Under Auxiliary Load and Speed Conditions", Trans. ASME, J. Basic Eng., Series D, Vol. 82, No. 2, June 1960, pp 309-320.

TABLE 2. ASSUMED BEARING DESIGN CONDITIONS

Parameter		Bearing Type 7955
Ball Diameter	m(in)	.012 (.500)
Pitch Diameter	m(in)	.081 (3.19)
Contact Angle	Degrees	20.5
Inner Race Curvature		.53
Outer Race Curvature		.53
Number of Balls		13
Speed	RPM	30,000

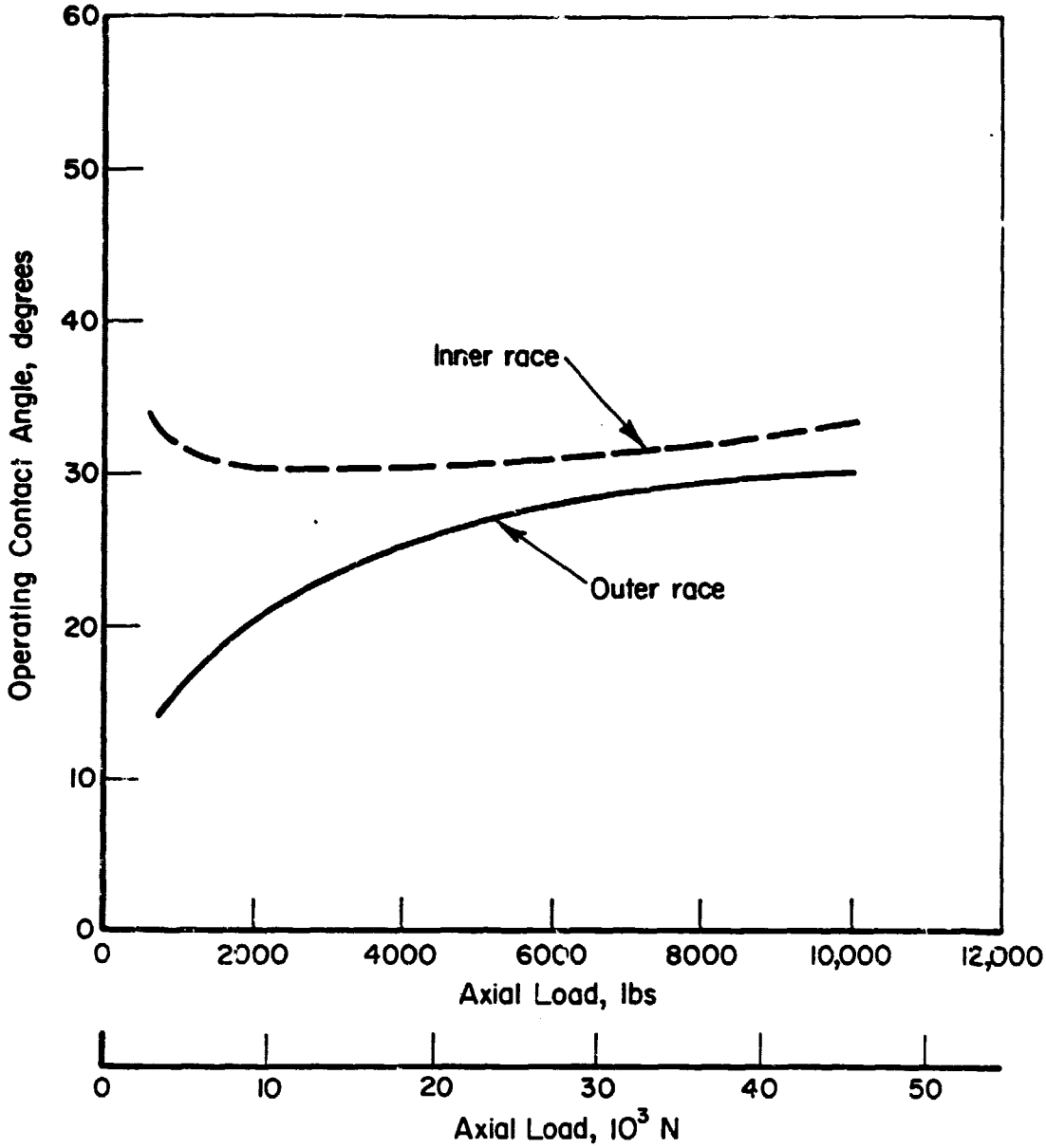

FIGURE 13. EFFECT OF AXIAL LOAD ON CONTACT ANGLE IN BEARING

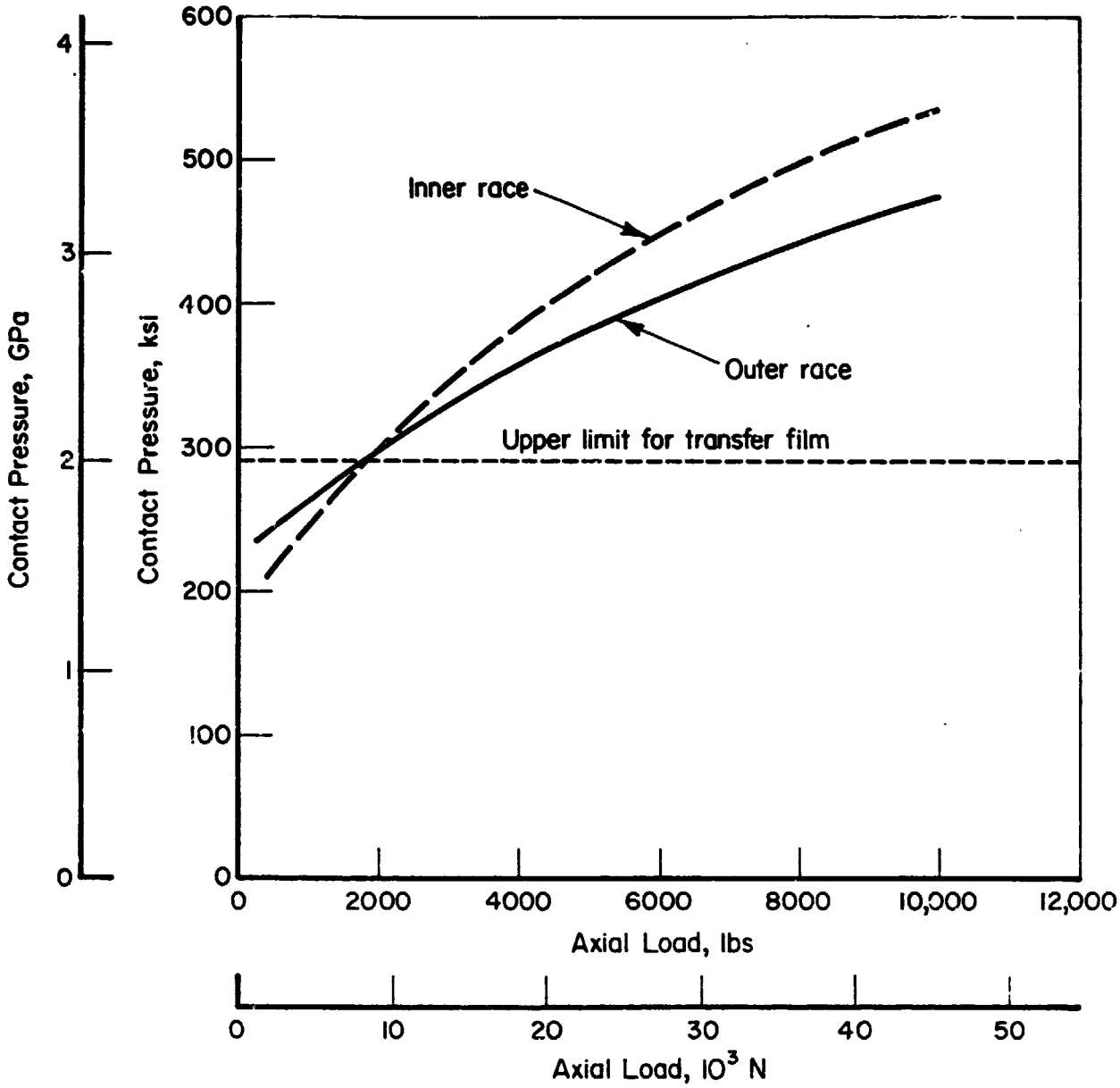

FIGURE 14. EFFECT OF AXIAL LOAD ON BEARING STRESS

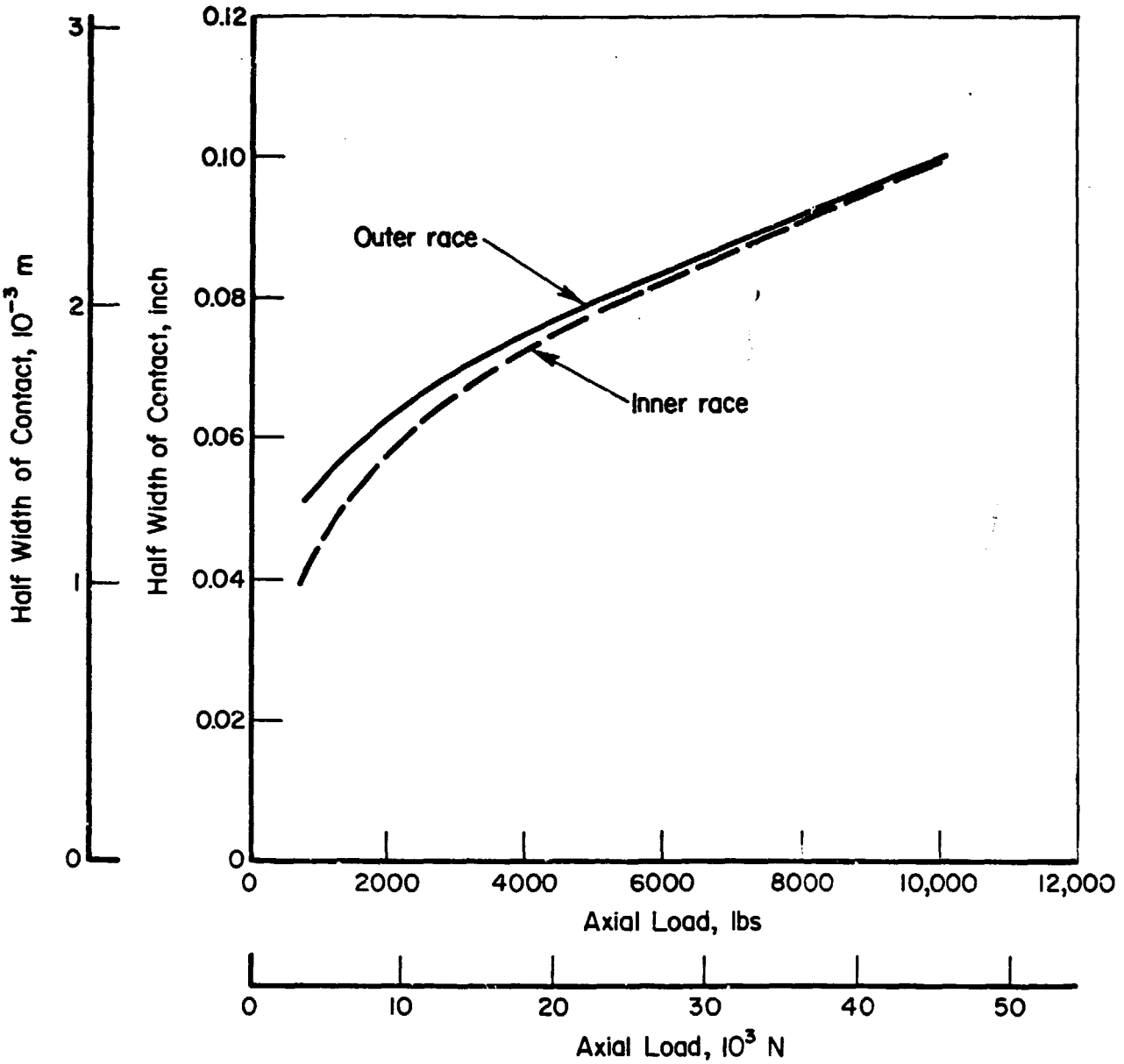

FIGURE 15. EFFECT OF AXIAL LOAD ON CONTACT WIDTH

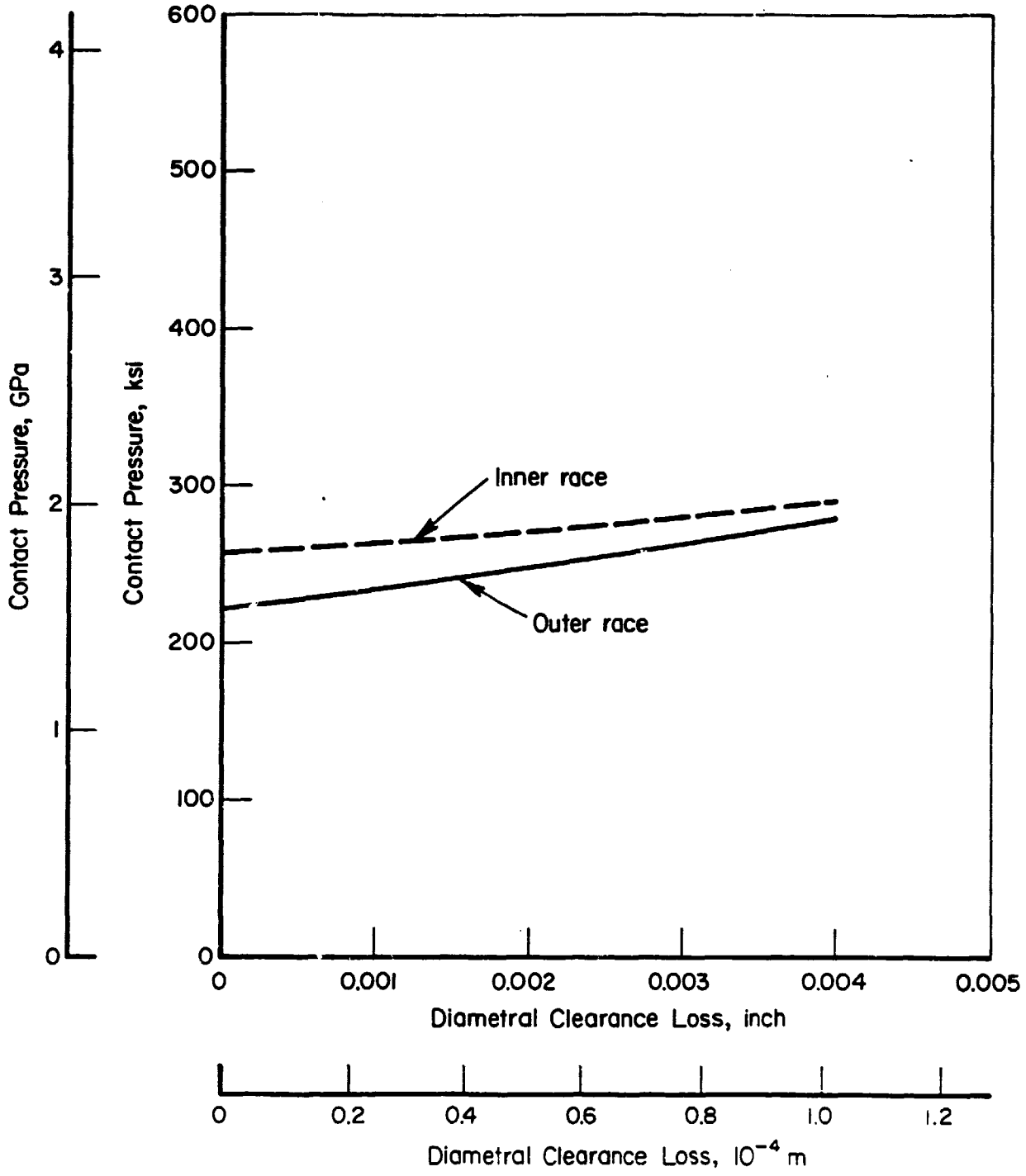

FIGURE 16. EFFECT OF LOSS OF DIAMETRAL CLEARANCE ON CONTACT STRESS - 850 POUNDS AXIAL LOAD

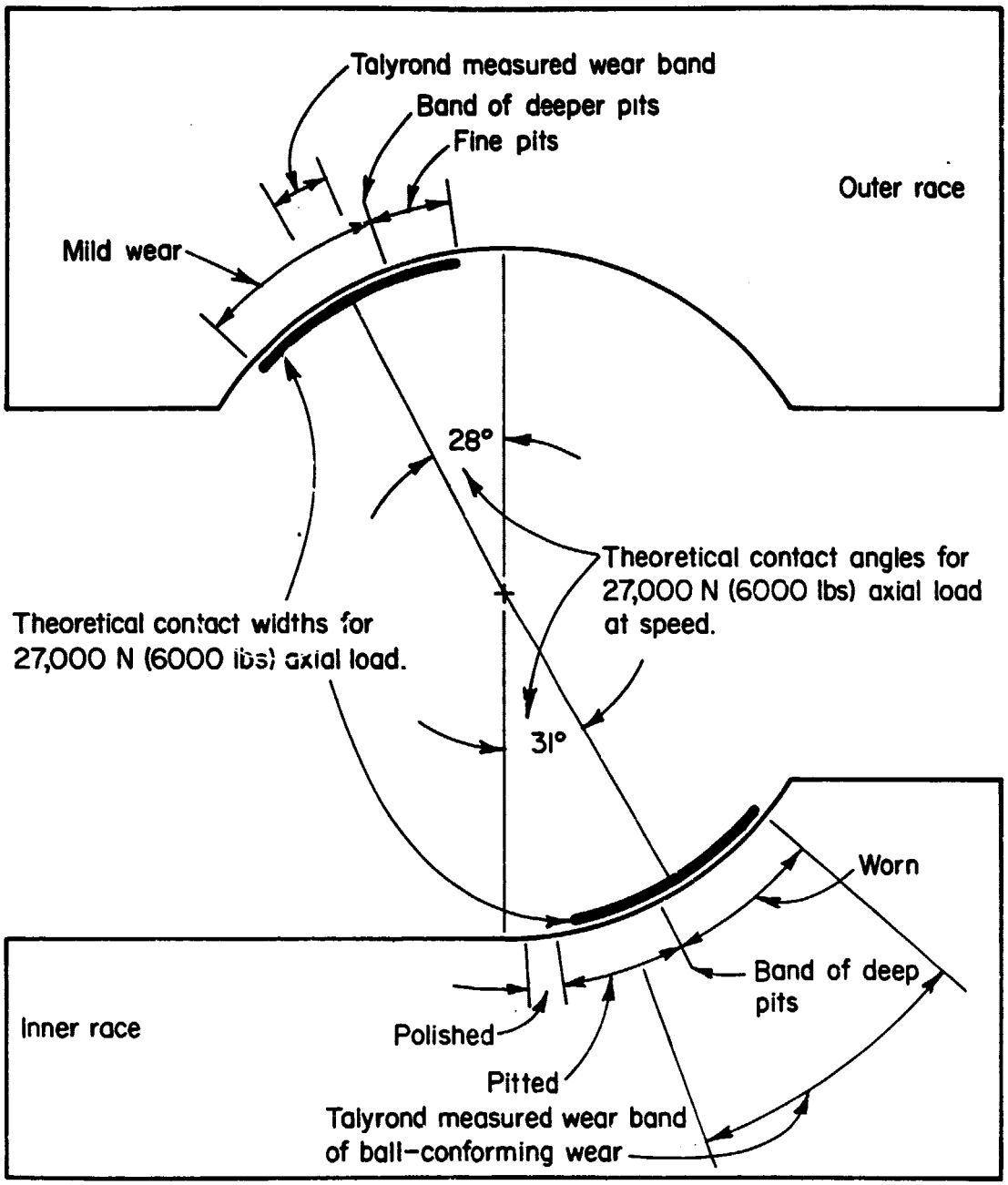

FIGURE 17. COMPARISON OF LOCATION OF ACTUAL BALL CONTACT LOCATIONS WITH THEORETICAL PREDICTIONS ON BEARING 8517903

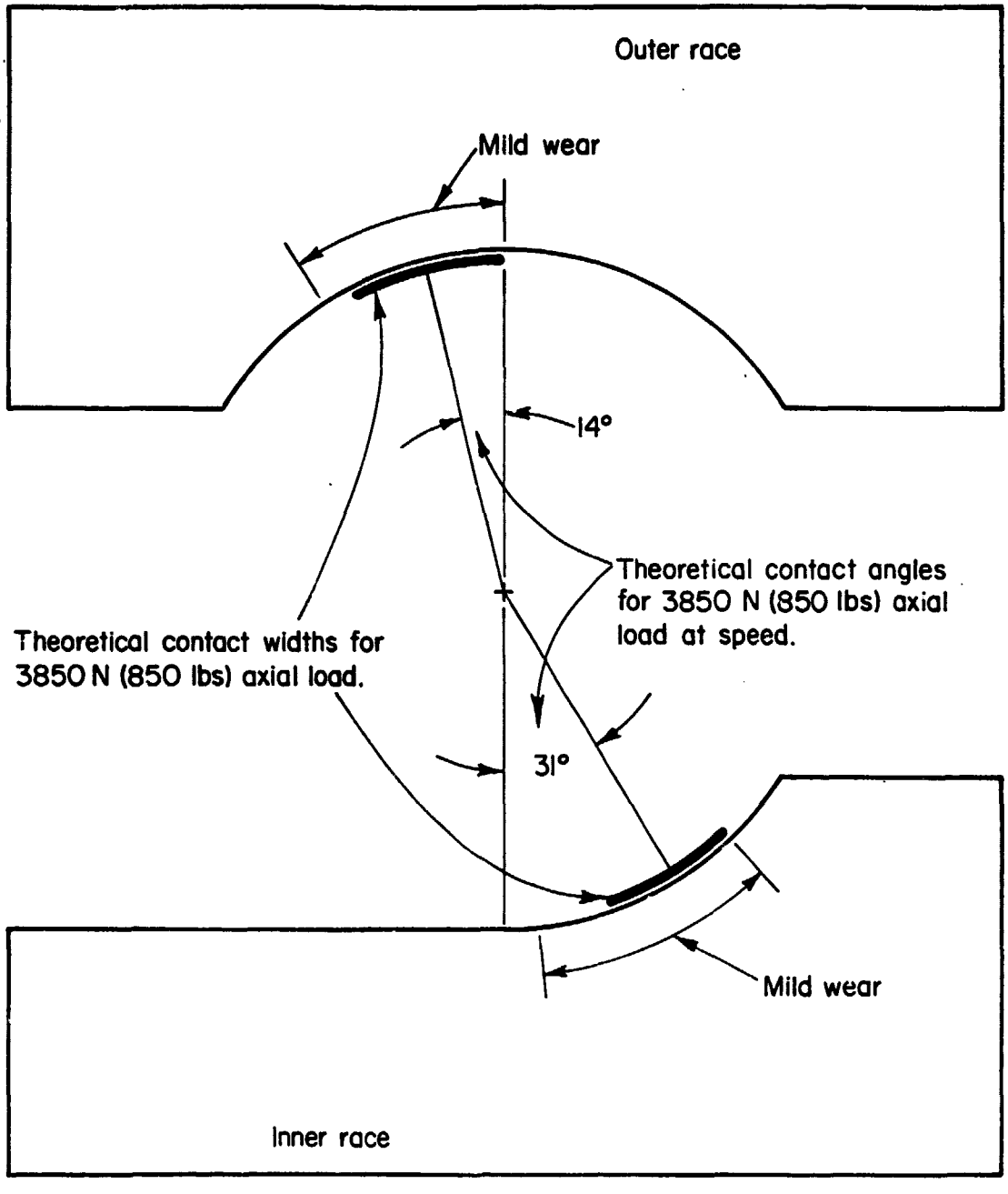

FIGURE 18. COMPARISON OF LOCATION OF ACTUAL BALL CONTACT LOCATIONS WITH THEORETICAL PREDICTIONS ON BEARING 8517900

In Figure 17, the locations of the predicted ball contact paths are seen to coincide quite well with the measured locations for axial load of approximately 27,000 N (6000 pounds). The small-circle banding of the balls probably resulted from contact with the chamfer on the inner race, which corresponded fairly well to the average location of the bands (not shown in Figure 17).

In Figure 18, the wear patterns on bearing 8517900 indicate that the normal axial preload of 3,800 N (850 pounds) was probably not exceeded for any significant period of time during operation of this bearing. The wider contact areas on both races resulted from start-up operation when the contact angle operates near the 20-degree design angle. As the bearing reaches operating speed, the contact angles change to those shown in Figure 18, thus explaining the wider wear areas, especially on the inner race.

The results of these measurements and calculations show that the bearing pair had a strong axial load applied against the 8517903 inner race, which was resisted by the outer race of that bearing. Since the outer race is designed to be able to respond to axial loads, by moving axially, either the outer race was restricted from doing so because of mechanical interference or the total limit of travel was reached.

DISCUSSION

There are many possible reasons for a bearing to fail to perform its required function for an acceptable period of time. The two most common causes of failure are fatigue of the bearing steel and inadequate lubrication.

Fatigue Considerations

In 1947, Lumbert and Palmgren published a theory for the failure distribution of ball and roller bearings. This theory is summarized by Coy, et al. in NASA TND-8362 (December 1976). Basically, the theory stated that bearing life can be expressed as

$$L_{10} = \left(\frac{K_1 z_o^{\ h}}{T_o^{\ c} \ V} \right)^{1/e} , \qquad (1)$$

where L_{10} = Life in millions of stress cycles (based on 90% survival)

$K = 3.58 \times 10^{56}$ (based on 52100 steel, English units)

$e = 1.11$

$h = 2.334$

$c = 10.334$

V = stress volume (z_o w)

w = semi-width of rolling track

z_o = depth of maximum shear stress

T_o = maximum shear stress

ℓ = length of rolling track.

Using the case postulated in Figure 17, a 27,000 N (6000 pounds) axial load on bearing 8517903,

$z_o = 40$ inches

$T_o = 140{,}000$

$\ell = 8.5$ inches

$V = .027$ cubic inches

so

$L_{10} = 33$ million cycles

or 3 hours of bearing operation. The L_1 Life (99% survival) can be computed to be

$L_1 = 20$ minutes.

This implies that bearing failure due to fatigue is highly likely with the high axial load. Bearing life could also be considerably diminished by the surface dents which serve as initial failure points. It is mandatory that efforts be made to insure freedom of axial motion of the bearing and thereby prevent such high axial loads if any realistic life of the bearings is to be achieved.

Lubrication Effects

As we discussed in our November 1978 report, bearing performance depends heavily on the presence of some type of lubricant between the balls and races. There are two general types of lubricant films normally factored into bearing design: hydrodynamic and boundary. Hydrodynamic lubrication occurs as a result of the hydrodynamic action of the lubricant (normally a

liquid) which forces a full film layer to form between ball and races. Under good hydrodynamic lubrication, a bearing will last indefinitely. Boundary lubrication occurs as a result of a chemical reaction between the lubricant, the lubricant additive, or dissolved oxygen in the lubricant with the metal surfaces. The "boundary films" are only a few monolayers thick and afford protection against cold welding of the surfaces. Both hydrodynamic and boundary films are necessary for good bearing performance. The hydrodynamic films keep the surfaces apart and the boundary films provide a back up during start up or during partial full film loss due to high asperities, system dynamics, inadvertent high load or debris in the lubricant.

Since cryogenic fluids which are probably gaseous in ball-race contact regions are not considered to be suitable lubricants, the pump bearings must be lubricated by some other mechanism. This mechanism appears to be a pseudo-transfer film (retainer to ball) process. Such films have been observed in our examination of the bearing. The use of transfer films in high-speed, high-load applications is beyond the art of bearing technology and little is known of their assets or limitations. One limitation that is known is the allowable stress level. This level is on the order of 2 GPa (280,000 psi) maximum Hertz stress. Above this stress, the bearing elements are operating in metallic con t. A second limitation is the supply rate of the lubricant by the retainer wear process in the ball pockets. If this process is too high, the retainer wears out prematurely. If it is too low, inadequate lubrication results. With the very small amount of retainer wear measured, the wear rate should be increased.

Under poor lubrication conditions, considerable frictional forces between the balls and races will occur as a result of the ball spin on the non-controlling race. This friction force alters not only the surface shear stresses, but also the whole subsurface stress patterns. Under very high friction ($f \approx .2$) the maximum shear stress is on the surface.

Assuming Equation (1) is valid, it can be seen that

$$L_{10} \propto z_o^{1.2} \quad , \tag{2}$$

where, as mentioned before, z_o is the depth to the maximum shear stress. Obviously, as the maximum stress approaches the surface, bearing life approaches

"zero." Relative bearing life is shown as a function of coefficients of friction in Figure 19. The relationship between z_o and friction is modeled after the work of Smith and Lui* and, realistically, is only rigorous for line contacts (plain strain) problems.

One interesting observation from the stress analyses is that a friction coefficient level of around 0.1 or greater, two peaks in shear stress curve occur. The first peak is at the surface and the second peak is near the normal depth. The surface shear stress peak becomes the largest at $f < 0.2$. However, it is interesting to speculate the surface initiated fatigue may well be occurring for $0.1 < f < 0,2$ and may be responsible for the shallow fatigue pit such as shown in Figure 1(a).

The above calculations indicate that in order to optimize bearing performance, it is mandatory that, as a minimum, adequate transfer film lubrication must be maintained. This means that the stresses in the bearing must be kept below 2 GPa (280,000 psi). With the current configuration, achieving this stress level is very difficult as shown in Figure 14. Computer runs were made for other bearing configurations involving minor changes in curvature and contact angles from the current design. The results of these runs are shown in Figure 20. It appears that reducing the curvature (both inner and outer race) from 0.53 to 0.52 could greatly enhance the probability for bearing survival. Note however, that changing the contact angle does not appear to improve the stress levels. Full bearing tests should be conducted with the bearing of 0.52 curvature to check the validity of this recommendation.

Measuring Units

Since the bearing drawings and all input data provided by NASA were in English units, all measurements and calculations were performed in English units. Therefore, the SI units presented in this report were converted from English units. Data on which this report is based are located in Battelle Laboratory Record Book No. 34405.

---

*Smith, J.O., and Liu, Chang Keng, "Stresses Due to Tangential and Normal Loads on an Elastic Solid with Applications to Some Contact Stress Problems", Trans. ASME, J. App. Mech., June 1953, pp 157-166.

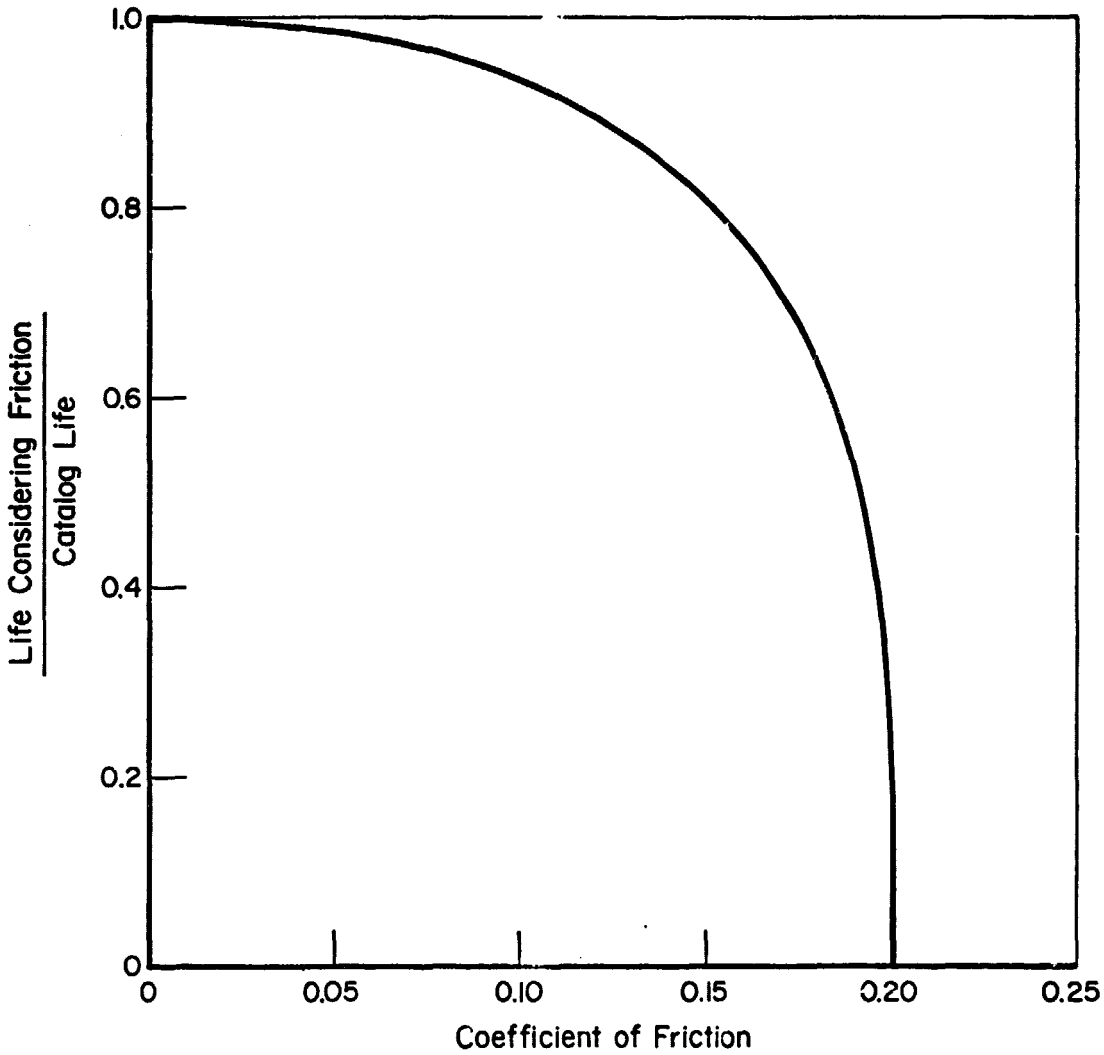

FIGURE 19. EFFECT OF FRICTION ON LIFE CALCULATIONS FOR ROLLING ELEMENT BEARING

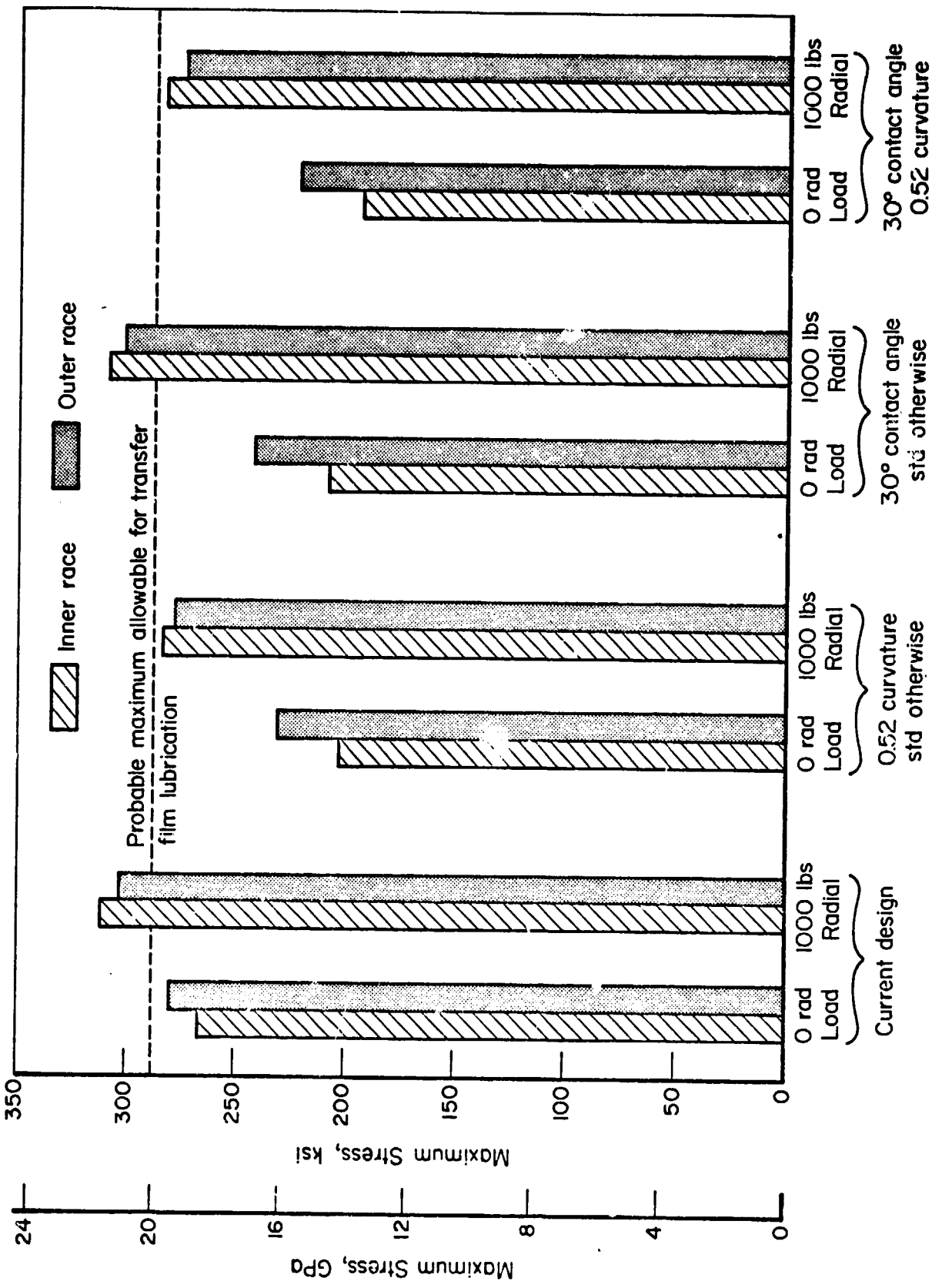

FIGURE 20. EFFECT OF MINOR DESIGN CHANGES ON BEARING CONTACT PRESSURES